35th Annual International Conference of the IEEE EMBS
Osaka, Japan, 3 - 7 July, 2013

Biomechanical Analysis for the Epidural Needle Insertion*

K. Furuya, K. Naemura, *member, IEEE*, K. Nagai, N. Okubo, H. Saito

Abstract— **In order to test the hypothesis about reduction in the deformation of the ligamentum flavum due to tension inside the ligamentum flavum, nonlinear finite element (FE) analysis was employed. As a preliminary analysis of natural tissue, nonlinear FE analysis was applied to a rubber plate. Assuming that the rubber is third-order Mooney–Rivlin model, the analysis and the experimental curves overlap with each other until pierced point. The maximum major strain calculated by FE analysis was feasible to predict pierced point. To apply nonlinear FE analysis for the porcine ligamentum flavum, the Mooney–Rivlin coefficient of the porcine ligamentum flavum was identified from the tensile test data. Assuming that the sharp bar pierced the ligamentum flavum when the maximum major strain reached a constant value, the required displacement became shorter by 1.0mm by applying the initial tension.**

Key words: **Nonlinear finite element analysis, Mooney-Rivlin model, Maximum major strain, Ligamentum flavum**

I. Introduction

Epidural anesthesia is widely employed because it allows the patient to control analgesia after surgery [1][2], and because it has a variety of benefits compared with general anesthesia [3]. Needle insertion is necessary to introduce a catheter into the epidural space. Anesthesiologists cannot see the epidural space or the location of the needle tip inside a patient's body. The loss-of-resistance method is a kind of force feedback technique to identify when the needle tip reaches the epidural space. Acquiring the epidural needle insertion technique requires experience, and anesthesiologists who are not well skilled can miss the needle insertion, resulting in complications such as insufficient analgesia, sanguineous puncture, accidental dural puncture, and unsuccessful catheter placement. Meyer-Bender evaluated the incidence of immediate complications following 7958 non-obstetrical epidural anesthesia sessions, and identified patient- and maneuver-related risk factors [4]. Perforation of the dura mater was seen in 123 cases (1.6%). Dural puncture was more frequent in older patients. Neither spinal level, gender, height nor body mass index (BMI) influenced the occurrence of dural puncture. The cause of accidental dural puncture remains unclear.

As demonstrated in our previous porcine study [5], the ligamentum flavum deforms up to 3 mm before the needle tip reaches the epidural space. If deformation of the ligamentum flavum could be reduced, the number of dural punctures would be greatly decreased. The authors hypothesized that tension inside the ligamentum flavum generated by arching the spine would reduce deformation of the ligamentum flavum during epidural needle insertion. The effect of arching the spine during the epidural needle insertion was examined by experiments using porcine spines and a small retractor [6]. To simulate the arching spine, the width of the ligamentum flavum was enlarged by the retractor, and deformation of the enlarged ligamentum flavum before the needle puncture was decreased in comparison with the natural ligamentum flavum. In the porcine spine experiments, deformation of the ligamentum flavum during the needle insertion could not be compared between the natural and the enlarged ligamentum flavum of the same specimen due to the needle puncture. We employed finite element analysis to test the hypothesis about reduction in the deformation of the ligamentum flavum due to tension inside the ligamentum flavum. In the current study, we performed 1) a feasibility study of the use of finite element analysis to examine whether an elastic rubber plate could suitably simulate the experimental results, and 2) a deformation simulation study of the porcine ligamentum flavum from tensile test data.

II. Nonlinear Finite Element Analysis of Rubber Plate

As a preliminary analysis of natural tissue, nonlinear finite element (FE) analysis was applied to a rubber plate. The rubber plate is homogeneous and thus is easier than non-homogeneous material like natural tissue such as the ligamentum flavum to use to confirm the accuracy of analysis. The purpose of this analysis was to show that the required displacements to pierce the rubber plate can be predicted by nonlinear FE analysis, and the displacement can be reduced by increasing the tension of the rubber plate.

A. Experiment

Figure 1 shows the experimental equipment for pricking a rubber plate. The rubber plate was fixed by a clamp, and the fixed tension of the clamp could change to allow the plate to slide. The rubber plate was 30 mm high x 60 mm wide x 3 mm thick. Hardness of the rubber was 65 shore-A. The rubber plate was under pricked load with a sharp bar-like hypodermic needle. The top of the sharp bar was conical, and the dimension is shown in Fig. 2. The displacement of the sharp bar was controlled to within 6 mm/s by an actuator, as shown in Fig. 1. The right side of Fig. 1 shows the deformed rubber plate under the pricked load. The reaction force from the rubber plate to the bar was measured by using a load cell.

*Resrach supported by KAKENHI (23592313)

K. Furuya is with Mechanical and Systems Engineering Department, Gifu University, Gifu, Japan. (phone: +81-58-2932625; fax: +81-58-2932491; e-mail: furuya@gifu-u.ac.jp).

K. Naemura is with Clinical Engineering Department, Tokyo University of Technology, Ota, Tokyo, Japan (e-mail: nae@stf.teu.ac.jp).

K. Nagai and N. Okubo are with Precision Mechanics Department, Chuo University, Bunkyo, Tokyo, Japan (e-mail: okubo@mech.chuo-u.ac.jp).

H. Saito is with Unisis Corporation, Arakawa, Tokyo, Japan(e-mail: h-saito@unisis.co.jp)

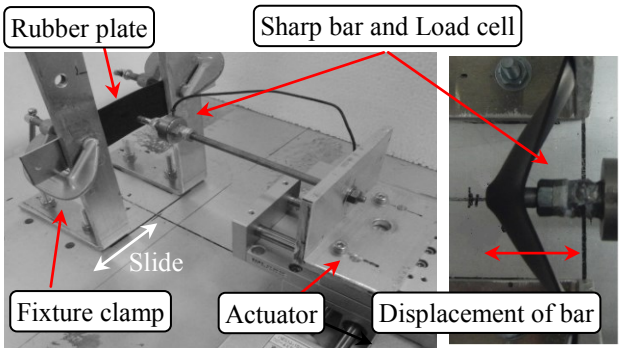

Fig. 1 Experimental equipment of pricking rubber plate.

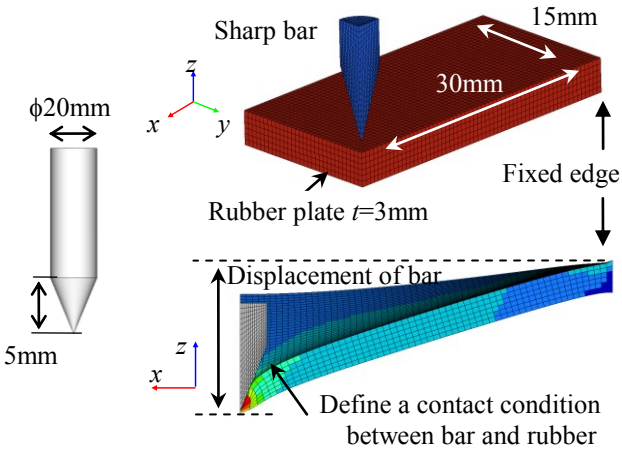

Fig. 2 Dimension of sharp bar and quarter FE model of the rubber plate and the sharp bar

B. FE analysis

The right side of Fig. 2 shows the FE model of the rubber plate and the sharp bar. Nonlinear analysis was done by a FE solver (MSC/Nastran sol600). The contact condition was defined between the sharp bar and the rubber plate. Assuming that the rubber is third-order Mooney–Rivlin model, which is an incompressible and nonlinear hyperplasic material, -Eq. (1) is adopted as a strain energy function W.

$$W = C_{10}(I_1-3)+C_{01}(I_2-3)+C_{11}(I_1-3)(I_2-3) + C_{20}(I_1-3)^2+C_{30}(I_1-3)^3 \quad (1)$$

where Ii is a strain invariant, and Cj is the coefficient of the Mooney–Rivlin material. Cj was obtained from the tensile test. In this analysis, Cj of the rubber plate shown in Table 1 published by JANCAE (Japan Association for Nonlinear CAE) were employed. These coefficients were identified from the 2 axial in-plane tensile test of Rubber 65 Shore A.

Table 1 Coefficients of Rubber 65 Shore A

C_{10}	C_{01}	C_{11}	C_{20}	C_{30}
4.512×10^5	3.428×10^4	-1.866×10^3	2.290×10^4	3.444×10^2

N/m^2 Unit. Reference from JANCAE

C. Results

First,we compared the analysis and the experimental result to confirm the accuracy of the nonlinear analysis. Figure 3 shows displacement of the bar and the reaction force from the rubber plate to the bar. The experimental curve had a peak at the displacement of 24.1mm. This peak shows that the sharp bar pierced the rubber plate. A curve of nonlinear FE analysis never expressed this peak, because the failure model between FE elements was not defined. However, the analysis and the experimental curves overlap with each other until pierced point of 24.1mm. The nonlinear FE analysis had sufficient accuracy.

The test showed that the required displacement to pierce the rubber plate can be predicted in nonlinear FE analysis, and that the displacement can be reduced by increasing the tension of the rubber plate. Figure 4 shows the curve of the maximum major strain in the FE model. The solid line indicates the FE analysis result shown in Fig. 3 (without initial tension). The dotted line indicates the FE analysis result with an applied initial tension of 5 mm. The initial tension was expressed by applying x-direction enforced displacement to the FE model edge, as shown in Fig. 2. The dotted line shows that the maximum major strain increased uniformly by applying initial tension. The solid line shows that the maximum major strain was 0.94 at the pierced point of 24.1 mm in displacement of the bar. Assuming that the sharp bar pierced the rubber plate when the maximum major strain reached 0.94 in the case of an initial tension of 5 mm, the required displacement to pierce the rubber plate is estimated to be 21.7 mm.

Figure 5 shows the experimental result with and without the initial tension of 5 mm. The gray dotted line indicates the experimental result with the initial tension. The dotted line had a peak at the predicted piecing point of 21.7 mm, and thus the assumption of piercing displacement based on the maximum major strain was appropriate.

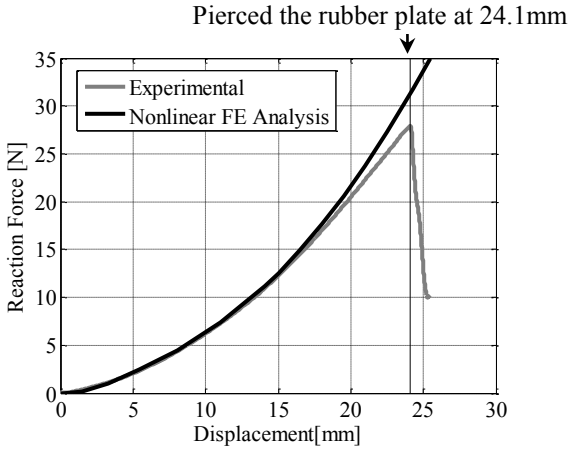

Fig. 3 Comparison of experiment and FE analysis on the relation between the displacements of the sharp bar and the reaction force from the rubber plate to the sharp bar.

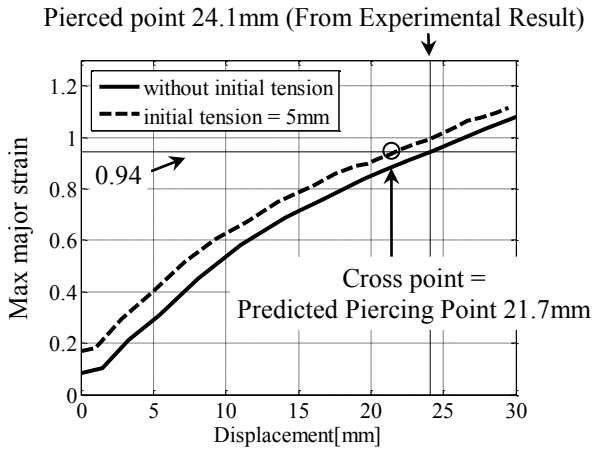

Fig. 4 FE analysis result of effect of the initial tension in the rubber plate on the relation between the displacements of the sharp bar and the maximum major strain.

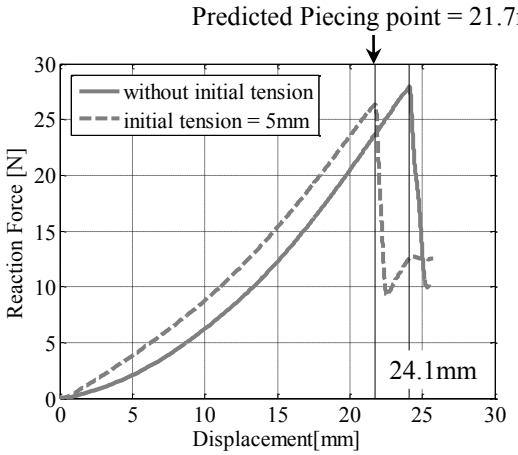

Fig. 5 Experimental waveforms on effect of the initial tension on the experimental curve between the displacement of the sharp bar and the reaction force.

III. Nonlinear FE Analysis of Ligamentum Flavum

A. Methods

Applying nonlinear FE analysis to porcine ligamentum flavum, the required displacement to pierce the porcine ligamentum flavum can be reduced by increasing the tension, like the case of the rubber plate.

To apply the FE analysis, it is necessary to identify the Mooney–Rivlin coefficient Cj of the porcine ligamentum flavum from the tensile test data. Figure 6 shows the test piece of porcine ligamentum flavum used in the tensile test. Sixteen test pieces were picked from the ligamentum flavum, and the cross section area of each was measured by using a CT scanner image. The porcine ligamentum flavum is non-homogeneous and anisotropic, so the test pieces were picked that those fiber directions became the same as much as possible. Gray lines in Fig. 7 show stress-strain curves of uniaxial tensile testing of the 16 test pieces. The nominal stress - nominal strain curves had the different values, although the pieces were picked that those fiber directions became the same. In this study, to investigate the qualitative characteristic of porcine ligamentum flavum, we used the averaged curve of the 16 test pieces for coefficient identification. The black line in Fig. 7 indicates the averaged curve. Table 2 shows the Mooney–Rivlin coefficient, Cj of the porcine ligamentum flavum. Only Mooney-Rivlin coefficients C_{10}, C_{20} had values, because the curve fitting was applied for uniaxial tensile testing data.

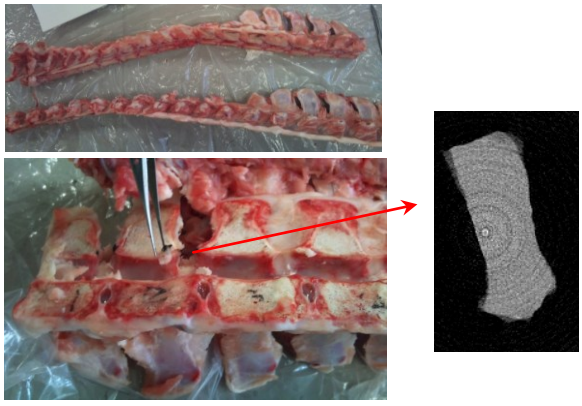

Fig. 6 Porcine ligamentum flavum and CT image of test piece

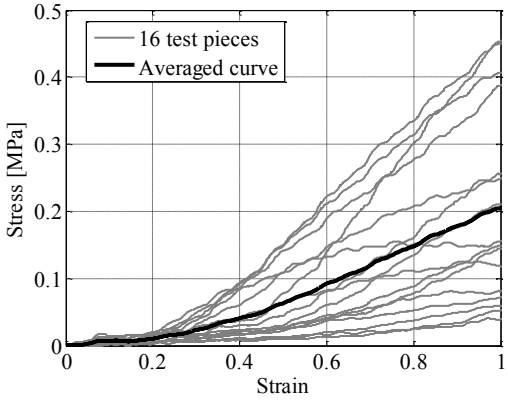

Fig. 7 Experimental stress strain curves of the porcine ligamentum flavum

Table 2. Coefficient of the porcine ligamentum flavum

C_{10}	C_{01}	C_{11}	C_{20}	C_{30}
7.63×10^3	0.0	0.0	4.46×10^3	0.0

N/m^2 Unit. Curve fitting from averaged stress-strain curve of uniaxial tensile testing

B. Results

The nonlinear FE analysis with and without initial tension was applied to the ligamentum flavum as it was to the rubber plate. The enforced displacement for applying tension was 1 mm. The resultant maximum major strain is shown in Fig. 8. Assuming that the sharp bar pierced the ligamentum flavum when the maximum major strain reached a constant value, Fig. 8 shows that the required displacement became shorter by about 0.5 to 1.0mm by applying the initial tension.

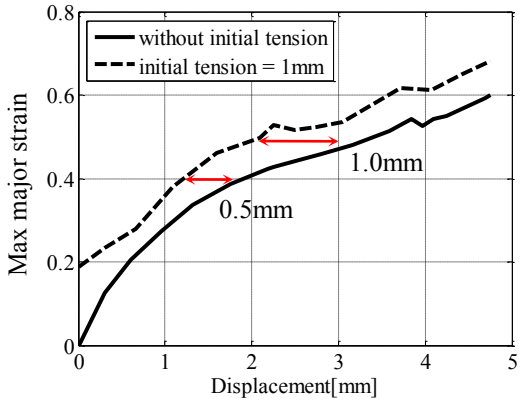

Fig. 8 FE analysis result on effect of the initial tension in the porcine ligamentum flavum on the relation between displacement of the sharp bar and the maximum major strain

IV. Conclusion

Nonlinear finite element analysis of the porcine ligamentum flavum with third-order Mooney–Rivlin model was feasible to calculate the maximum major strain and to predict piercing point.

References

[1] M. Sostaric, "Incisional administration of local anesthetic provides satisfactory analgesia following port access heart surgery", *Heart Surg Forum*, vol.8, no.6, E406-408, 2005

[2] K. Tokita, H. Tanaka, M. Kawamoto, O. Yuge, "Patient-controlled epidural analgesia with bupivacaine and fentanyl suppresses postoperative delirium following hepatectomy", *Masui*, vol.50, no.7, p.742-746, 2001.

[3] J. Y. Hong, S. J. Lee, K. H. Rha, G. U. Roh, S. Y. Kwon, H. K. Kil., "Effects of thoracic epidural analgesia combined with general anesthesia on intraoperative ventilation/oxygenation and postoperative pulmonary complications in robot-assisted laparoscopic radical prostatectomy", *J Endourol.*, vol.23, no.11, p. 1843-1849, 2009..

[4] A. Meyer-Bender, A. Kern, B. Pollwein, A. Crispin, P. M. Lang, "Incidence and predictors of immediate complications following perioperative non-obstetric epidural punctures", *BMC Anesthesiol.*, vol. 12, no.1, p.31, 2012.

[5] K. Naemura, H. Saito, "Needle Insertion Test by Porcine Ligamentum Flavum", *WC 2009, IFMBE Proceedings* 25/VI pp.28-31, 2009..

[6] K. Naemura, "Effect of Arching Spine on Deformation of the Ligamentum Flavum during Epidural Needle Insertion", *Proceedings of the 34th Annual International Conference of the IEEE EMBS* pp.3344-3347, 2012.